Ultrathin Layers and Supramolecular Architecture of Isopentylcellulose

M. Schaub, C. Fakirov, A. Schmidt, G. Lieser, G. Wenz, and G. Wegner*

Max-Planck-Institut für Polymerforschung, Postfach 3148, D-55021 Mainz, Germany

P.-A. Albouy

Laboratoire de Physique des Solides, Université Paris-Sud, F-91405 Orsay, France

H. Wu and M. D. Foster

Maurice Morton Institute of Polymer Science, University of Akron, Akron, Ohio 44325-3909

C. Majrkzak and S. Satija*

National Institute for Standards and Technology, Gaithersburg, Maryland 20899

Received September 6, 1994; Revised Manuscript Received September 16, 1994®

ABSTRACT: The characterization of multilayers from tri-*O*-isopentyl cellulose assembled by the Langmuir−Blodgett technique is described. The analysis of ultrathin films by X-ray reflection confirmed a homogeneous overall film quality but did not show any Bragg reflection. However, investigation of a superstructure in terms of an alternating multilayer sample from deuterated and nondeuterated isopentylcellulose ethers by neutron reflection revealed a perfectly periodic layer structure. The influence of the degree of substitution of the isopentylcellulose ethers on the formation and structure of multilayers was investigated as well. Multilayers of partially substituted isopentylcellulose exhibit a periodical film structure composed of double layers. The perfection of the films is not influenced by the residual OH functions. The in-plane structure of tri-*O*-isopentylcellulose multilayers was investigated by electron diffraction in transmission geometry. The cellulose ether forms a helix of 3-fold symmetry, and the helix axes are preferentially oriented parallel to the dipping direction. Upon annealing a three-dimensional crystalline film of layered structure is obtained in which the chains are packed in a monoclinic unit cell. The very small diameter of the cellulose derivatives of less than 10 Å/molecule in the layered superstructures and the observation that very perfect and homogeneously oriented multilayers are obtained by the Langmuir−Blodgett technique augment the toolbox of molecular architects interested in the rational construction of supramolecular architectures.

1. Introduction

The concept of using rigid-rod-like polymers, decorated with flexible alkyl side chains, to construct stable and homogeneous ultrathin films by the Langmuir−Blodgett (LB) technique has been applied to several types of macromolecules, e.g., phthalocyaninatopolysiloxanes (PCPS),[1,2] polyglutamates (PG),[3−5] and polysilanes (PSI).[6] The rigidity of these so-called hairy rod polymers guarantees that in Langmuir films every chain segment is in contact with the air/water interface so that the formation of loops and tails, which is a general problem in monolayers of conventional amphiphilic polymers, becomes impossible.[7] The formation of very homogeneous and compact monolayers is essential when one wants to assemble well-defined highly periodical multilayer structures. The alkyl side chains of the hairy rod polymers are in general designed to be noncrystallizing, so that formation of an inhomogeneous polycrystalline domain structure, as is usually found in conventional amphiphilic systems, is prohibited. Multilayers of hairy rods are, therefore, considered as molecularly reinforced liquids where rigid polymer backbones are embedded in a liquidlike matrix of alkyl chains.[8] This induces a fluidlike character which enables the incorporation of guest molecules or of covalently attached functional groups without destroying the regularity and homogeneity of the multilayers.[4,9,10]

Because of flow processes in the monolayer film at the air/water interface, in the course of the monolayer transfer and deposition to solid substrates the main axes of the rodlike polymers become preferentially oriented parallel to the dipping direction of the substrate. Therefore, it is possible to adjust the orientation of the polymer chains in consecutive layers just by changing the dipping direction.[11] A pictorial description of the spreading and transfer process as well as of the supramolecular architecture generally observed for multilayers of hairy rods is given in Figure 1. Hairy rod macromolecules have been demonstrated to substantially augment the toolbox of supramolecular architects and are most useful in the construction of complex architectures to be used in planar optics, as field-effect sensoric devices, as orientation layers in liquid crystalline displays, and for tunneling diodes; recent reviews are found in refs 9, 10, and 33.

Among the polymers that have been designed according to the hairy rod concept in order to construct regular ultrathin multilayers by the LB technique are alkylated cellulose derivatives,[12] which are the subject of the following report.

The spreading behavior of cellulose derivatives at the air/water interface like cellulose acetate and ethylcellulose have been investigated for more than 60 years.[13,14] However, transferable derivatives were not obtained before Kawaguchi et al. succeeded in transferring a monolayer of cellulose tridecanoate using a horizontal dipping method.[15] Investigations of multilayers from these cellulose derivatives by polarized FTIR spectros-

* To whom all correspondence should be addressed.

® Abstract published in *Advance ACS Abstracts,* January 15, 1995.

0024-9297/95/2228-1221$09.00/0

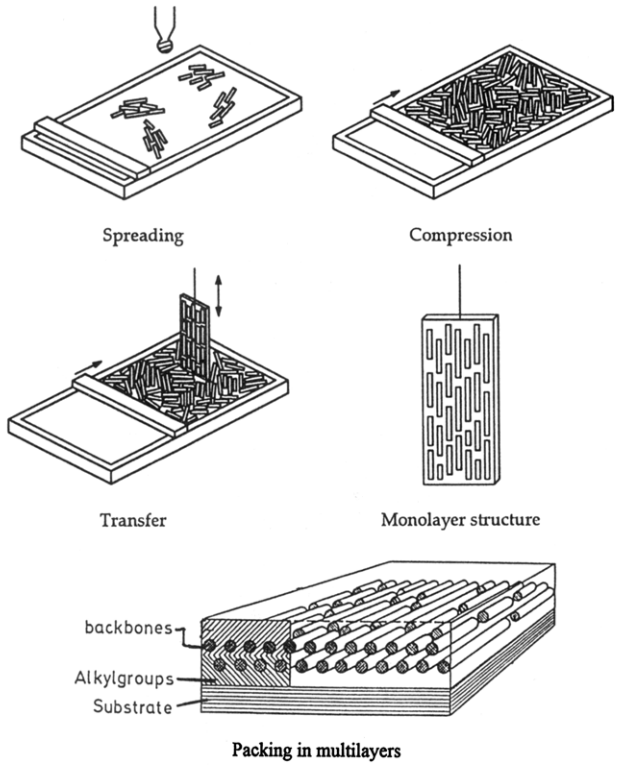

Figure 1. Schematic representation of the different steps in the construction of supramolecular layered architectures of hairy rod macromolecules by the LB technique and flow-induced in-plane orientation of the backbone elements to provide for a frozen-in nematic order in terms of a monodomain (idealized depiction) in each monolayer transferred.

copy and XPS revealed a film structure typical for amphiphilic systems: the hydrophobic side chains were oriented normal to the substrate plane and the cellulose backbone with the ester groups provided the hydrophilic parts.

It has also been shown that a different class of cellulose derivatives, namely, cellulose alkyl ethers with degrees of substitution (ds) near 3, form monolayers at the air/water interface that can be transferred onto solid substrates when the side chain length is in the range of 4–5 C atoms (e.g., tri-*O*-isopentylcellulose).[12,16] A detailed investigation of these systems indicated that the characteristic qualities of hairy rods like chain stiffness and side-chain flexibility are realized.[17] The very low monolayer thickness of less that 1 nm and the great structural variability which provides for the incorporation of functional groups in the side-chain matrix are of particular interest. A survey of possible applications of ultrathin polymer films assembled by the Langmuir–Blodgett technique is presented elsewhere.[18,19] In this context and particularly for applications of ultrathin cellulose ether films as membranes for separation purposes or in sensors, it may be necessary to vary the hydrophobicity of the multilayers or to induce functional groups into the polymer film.[19] Therefore, cellulose ethers incompletely etherified, that is with free hydroxyl functions, are interesting materials for LB multilayer assembly with respect to practical applications.

Chart 1 represents the chemical structure of the polymer systems of varying content of OH groups which are the subject of this paper. The sample IPC-*d* had all isopentyl residues perdeuterated.

Investigations of multilayer systems of these cellulose ethers by polarized FTIR spectroscopy had shown that the polymer main axes are aligned in the layer plane

Chart 1

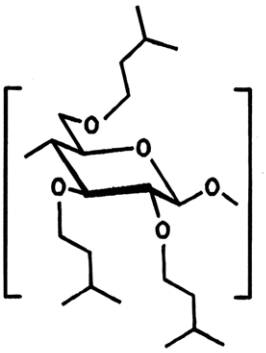

polymer abbreviation	degree of substitution (ds)
IPC3.0	3.0
IPC2.9	2.9
IPC2.7	2.7
IPC2.3	2.3
IPC-d	2.8

and parallel to the dipping direction of the substrate.[20] This being the only available information on the LB film structure from cellulose ethers, it was our intention to obtain further information about the layered films and the molecular packing of the cellulose ether chains within the multilayers and to investigate the influence of the degree of substitution on the film architecture. We used X-ray and neutron diffraction in reflection geometry and electron diffraction as the main tools.

These analytical methods have already been used to investigate the structure of multilayers of rodlike polymers. Investigation of PG, PCPS, or PS by X-ray or neutron reflectometry showed that freshly prepared samples have a perodical double-layer structure which may relax to a hexagonal structure on annealing.[5,6] Electron diffraction in transmission geometry revealed the oriented in-layer structure ad the dense packing of the polymer rods.[21]

Whereas diffraction patterns of thin films obtained by transmission geometry are similar to fiber patterns whose interpretation follows conventional rules, the reflectivity technique has only recently been applied to analyze the structure of ultrathin organic or polymer films.[22,23] The X-ray and neutron specular reflection results in complex diffraction patterns that reveal detailed information about the film quality and structure along the substrate normal.[22–25] Therefore, the basis of the reflectivity technique as applied here is outlined briefly in the following.

2. Reflectivity of X-rays and Neutrons

Diffraction of X-rays and neutrons in specular reflection geometry supplies information about the thickness, surface roughness, and electron density profile (scattering length density profile for neutrons respectively) of ultrathin film systems.[22–25] Additional information about packing regularity or interlayer diffusion can be

obtained by neutron reflectivity when layers of deuterated and nondeuterated materials are combined in a periodic multilayer structure.[5,26]

The reflection of X-ray or neutron radiation of a surface is determined by the refractive index n of the sample. When absorption effects can be neglected, the refractive index n is given by:[27]

$$n = 1 - \delta \tag{1}$$

where

$$\delta_x = \frac{1}{2\pi}\lambda^2 r_{el}\varrho_{el} \qquad \text{for X-rays}$$

and

$$\delta_n = \frac{1}{2\pi}\lambda^2\frac{b}{V} \qquad \text{for neutrons}$$

λ is the wavelength of the diffracted radiation, r_{el} the classical electron radius, ϱ_{el} the electron density, and b/V the scattering length density for neutrons. The refractive index which depends on the electron density, or for neutrons on the scattering length density, is always smaller than 1.

The amplitude $A(q)$ of reflected radiation can be calculated as a function of the scattering vector q by using a Fourier transform formalism, dynamical effects being neglected:[22,23]

$$A(q) = \frac{4\pi r_{el}}{q}\int_{-\infty}^{+\infty}\varrho_{el}(z)\exp(iqz)\,dz \tag{2}$$

$\varrho_{el}(z)$ is the electron density profile along the surface normal (z-direction) which describes the refractive index profile. This equation and the following equations are also valid for neutrons, if $r_{el}\varrho_{el}$ is substituted by b/V.

Partial integration results in

$$A(q) = i\frac{4\pi r_{el}}{q^2}\int_{-\infty}^{+\infty}\frac{d\varrho_{el}(z)}{dz}\exp(iqz)\,dz \tag{3}$$

The electron density profile $\varrho_{el}(z)$ of a multilayer film of N periods with periodicity d and overall film thickness E on a substrate can be modeled by

$$\varrho_{el}(z) = \varrho_p[\mathrm{erf}(z) + 1/2] + (\varrho_s - \varrho_p)[\mathrm{erf}(z - E) + 1/2] + \Delta\varrho_0(z)\sum_{n=1}^{N}\delta_D\left(z - nd + \frac{d}{2}\right) \tag{4}$$

ϱ_p and ϱ_s denote the average electron density of the polymer film and the substrate. $\Delta\varrho_0(z)$ is the electron density modulation of a periodical unit in the interval $(-d/2;d/2)$ and δ_D is the Dirac delta function. Roughness of the interfaces leads to error-function profiles of electron density (or scattering length density), if a Gaussian distribution of the interface position is assumed. The parameters σ_p and σ_s represent the roughness parameters of the air/polymer and polymer/substrate interfaces, respectively.

With the first and second term of (4) in (3) one obtains $A_1(q)$ which describes the amplitude of the beams reflected by the interfaces air/polymer and polymer/substrate.

$$A_1(q) = i\frac{4\pi r_{el}}{q^2}\left\{\varrho_p\exp\left(-\frac{q^2\sigma_p^2}{2}\right) + (\varrho_s - \varrho_p)\exp\left(-\frac{q^2\sigma_s^2}{2}\right)\exp(iqNd)\right\} \tag{5}$$

The third term of (4) in (2) leads to $A_2(q)$ which describes Bragg reflection at the periodic multilayer structure.

$$A_2(q) = \frac{4\pi r_{el}}{q}F(q)\exp\left(i\frac{qNd}{2}\right)\frac{\sin(qNd/2)}{\sin(qd/2)} \tag{6}$$

The structure factor $F(q)$ of a repeating unit in the periodical multilayer is given by

$$F(q) = \int_{-d/2}^{d/2}\Delta\varrho_0(z)\exp(iqz)\,dz \tag{7}$$

The electron density modulation of a repeating unit $\Delta\varrho_0(z)$ may be represented by a cosine series if $\Delta\varrho_0(z)$ is assumed to be centrosymmetric, with the coefficients ψ_k:

$$\Delta\varrho_0(z) = \sum_{k=1}^{\infty}\psi_k\cos\left(\frac{2k\pi}{d}z\right) \tag{8}$$

The overall intensity $I(q)$ of the reflected beam is given by

$$I(q) = |A_1(q) + A_2(q)|^2 = A_1(q)A_1^*(q) + A_2(q)A_2^*(q) + A_1(q)A_2^*(q) + A_1^*(q)A_2(q) \tag{9}$$

$I(q)$ consists of a contribution caused by interferences of the reflection from the two interfaces which leads to periodic intensity modulations, so-called Kiessig fringes (first term of eq 9). The Kiessig fringes allow the determination of the whole film thickness $E = Nd$ and the roughness parameters σ_p and σ_s of the air/polymer and polymer/substrate interfaces. The second term of (9), which is caused by Bragg reflection from the periodic multilayer structure, enables the determination of the square of $F(q)$. The structure factor $F(q)$ and therefore the electron density profile of a repeating unit $\Delta\varrho_0(z)$ can be determined without losing information about the sign due to the interference terms $A_1A_2^* + A_1^*A_2$.[23]

In a typical reflectometry experiment X-ray or neutron radiation is reflected from a multilayer system under a distinct angle θ, while the intensity $I(q)$ of the reflected radiation is detected (Figure 2). The reflection curve is presented as $I(q)$ or $(I(q)\,q^2)$ plotted against the scattering vector q. A theoretically calculated typical reflectivity curve with Kiessig fringes caused by interface reflection and a first-order Bragg reflection is shown in Figure 2. It represents a multilayer system consisting of 15 layers with a periodicity d of 35 Å, i.e., with an overall film thickness E of 525 Å and a ψ_1 of 0.03.

By fitting a reflection curve (X-ray or neutron) of an LB multilayer according to (5)–(9), it is possible to obtain the important film parameters: E, d, σ_p, σ_s, ψ_k. The determination of the coefficients ψ_k permits with (8) the evaluation of the electron density profile (scattering length density profile for neutrons) of the individual monolayers in the assembly along the surface normal. Therefore, reflectivity techniques are powerful

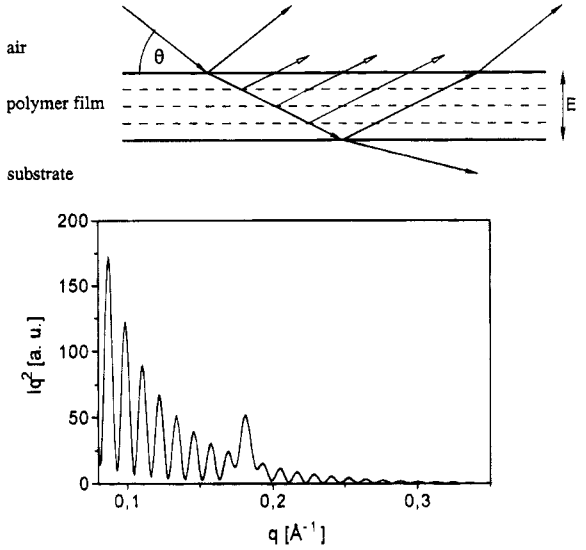

Figure 2. Schematic representation of X-ray or neutron reflection from a LB multilayer system, resulting in a typical reflection curve. The reflection curve is calculated for a multilayer system of 15 layers with a periodicity of 35 Å, i.e., overall film thickness E = 525 Å, surface roughness of 5 Å, and a Fourier coefficient ψ_1 = 0.03.

analytical methods to investigate the vertical structure of LB multilayer systems.

3. Experimental Section

Synthesis and Characterization. Tri-*O*-isopentyl Cellulose. General Procedure.[28] Sodium hydroxide powder and 3-methylbutyl bromide was added in a desired excess to a degassed solution of 1 g of cellulose acetate (Aldrich; ds = 2.34, average degree of polymerization 150) in 50 mL of dry DMSO. After it was stirred for 6 days at room temperature under nitrogen, the mixture was poured into 400 mL of water. The cellulose ether was isolated by extraction with methylene chloride and purified by repeated dissolution in methylene chloride followed by precipitation in methanol. The degree of substitution of the isopentylcellulose was found to be 2.9, 2.7, and 2.3 for the reactions with 12-fold, 8-fold, and 3-fold molar excess of the reagents sodium hydroxide and alkyl bromide per cellulosic OH group, with an average yield of 85%. IR spectroscopy confirmed that no residual acetate groups were present. Using membrane osmometry, an average degree of polymerization of 73 was determined.

To obtain a completely substituted isopentylcellulose ether, the remaining free hydroxyl functions were alkylated by dissolving 0.8 g of isopentylcellulose of ds 2.9 (IPC2.9) in a mixture of 20 mL of toluene and 5 mL of THF. A total of 1.12 g of potassium *tert*-butylate and 1.51 g of 3-methylbutyl bromide were then added. After it was stirred for 10 h at room temperature under nitrogen, the mixture was poured into 400 mL of water. The precipitate was purified by dissolving it in methylene chloride. Reprecipitation in methanol gave 0.43 g (52.5%) of tri-*O*-*isopentylcellulose* of ds = 3.

The ds was confirmed by chemical analysis, ^{1}H NMR spectroscopy, and reductive cleavage.[29] Anal. Calcd for $C_{21}H_{40}O_5$: C, 67.7; H, 10.82; O, 21.47. Found: C, 68.19; H, 10.71; O, 20.73. ^{1}H-NMR (300 MHz, toluene-d_8, 100 °C): δ 4.58 (d, J = 6.8 Hz, 1H, 1), 4.12 (m, 1H, 2′), 3.93 (m, 4, 6), 3.82 (m, 6, 1′), 3.76 (m, 1′), 3.57 (m, 2H, 1′), 3.36 (m, 2H, 3, 5), 3.12 (t, J = 6.8 Hz, 1H, 2), 1.78 (m, 3H, 3′), 1.67−1.56 (m, 6H, 2′), 0.95 (dd, J = 7.3 Hz, 18H, 4′). ^{13}C-NMR (75.5 MHz, 1,1,2,2-tetrachloroethane-d_2, 100 °C): δ 102.69 (1), 84.03 (2), 82.87 (3), 77.11 (5), 76.13 (4), 71.67 (1′), 70.22 (1′), 69.67 (6), 39.67 (2′), 39.25 (2′), 25.48 (3′), 25.34 (3′), 23.15 (4′), 23.0 (4′).

Isopentyl-d_{11}-cellulose (IPC-d). For the preparation of an isopentylcellulose ether with perdeuterated side chains, 0.35 g of cellulose acetate was dissolved in 18 mL of dry DMSO and 1.48 g of sodium hydroxide powder and 5.9 g of 3-methylbutyl-d_{11} bromide were added. The reaction was carried out as described above.

3-Methylbutyl-d_{11} bromide was synthesized according to a procedure described in ref 30. A material characterized as isopentyl-d_{11}-cellulose of ds = 2.8 was obtained as determined by chemical analysis. Anal. Calcd (ds = 2.8): C, 67.0; H, 10.7; O, 22.3. Found: C, 67.39; H, 9.94; O, 20.99. ^{1}H-NMR (300 MHz, 1,1,2,2,-tetrachloroethane-d_2, 100 °C): δ 4.35 (d, J = 7.5 Hz, 1H, 1), 3.68 (m, 3H, 4, 6), 3.18 (m, 2H, 3, 5), 2.93 (t, J = 7.5 Hz, 1H, 2), 1.61 (m, 3′), 1.45 (m, 2′), 1.38 (m, 2′), 0.83 (m, 4′).

Multilayer Preparation. A solution of 3 mg of polymer in 10 mL of chloroform (Merck, UVASOL) was spread onto a water surface of a Lauda FW-1 film balance (subphase temperature 20 °C). The monolayer was compressed to a surface pressure of 17 mN/m and transferred to hydrophobic glass or silicon substrates in a Y-type deposition (dipping speed 1 cm/min) with a transfer ratio of 100% during down- and upstrokes. Alternating layers were prepared using two Lauda FW-1 film balances simultaneously.

Silicon wafers and glass slides were cleaned with $CHCl_3$ in an ultrasonic bath for 15 min, then treated with a mixture of H_2O_2 (30%)/NH_4OH (25%)/water (1:1:5) for 30 min at 80 °C, rinsed with pure water, and exposed for 15 min to an Ar/O_2 plasma.

Hydrophobization of glass slides was achieved by treatment with a solution of hexamethyldisilazane in $CHCl_3$ (20%) at 50 °C for 30 min. Silicon wafers were hydrophobized by dipping in an aqueous solution of NH_4F (25%) for 30 s.

The samples for the electron diffraction were prepared by using thoroughly cleaned, though not hydrophobized, glass slides coated with a thin film of carbon as a substrate. After the multilayer deposition the carbon film was floated off on water and picked up on 300-mesh copper grids. The crystallization of the multilayer system was achieved by annealing the sample for 12 h at 150 °C in vacuum.

Measurements. X-ray reflection was performed with a Philips PW 1820 powder goniometer equipped with a curved graphite analyzer and mounted on a conventional X-ray generator (copper anode, $\lambda_{K\alpha}$ = 1.542 Å; experimental resolution, 0.001 85 $Å^{-1}$). The minimum angle of incidence (-2θ = 0.4°) was determined by the maximum capacity of the detector so that an analysis near the edge of total reflection was not permitted. The experimental reflectivity curve was analyzed by comparison with a simulated pattern of the multilayer system, using the Fourier transform method outlined in section 2.

Neutron reflection was performed at the neutron source of the National Institute of Standards and Technology (Gaithersburg, MD) with a neutron wavelength of 2.35 Å and a ^{3}He tube as the detector. For a detailed specification of the neutron reflection experiment, see ref 31. Simulation of the experimental curve was carried out using the Fourier transform method, considering dynamical effects at low angles of incidence.

Electron diffraction measurements were performed on both a Philips CM 12 and a Zeiss EM 912 Ω electron microscope operated at an accelerating voltage of 120 kV. The microscopes are equipped with eucentric goniometers, allowing sample tilting in a range of ±60°. The extreme sensitivity of the polymer to radiation damage required application of a cold stage, which allowed one to investigate the specimen at liquid nitrogen temperatures, except for the cases when for the purposes of structure determination a rotation holder was used.

4. Results and Discussion

Synthesis and Characterization of Cellulose Isopentyl Ether. The synthesis of cellulose alkyl ethers starting from cellulose acetate has been reported by Isogai et al.[28] We used the same method only slightly modified in order to prepare cellulose isopentyl ethers of different ds.[16]

Reaction of cellulose acetate dissolved in dimethyl sulfoxide with an excess of 3-methylbutyl bromide and sodium hydroxide gave isopentylcellulose with a ds of 2.9. A cellulose ether of ds of 2.7 was obtained with an 8-fold and of 2.3 with a 3-fold stoichiometric excess of

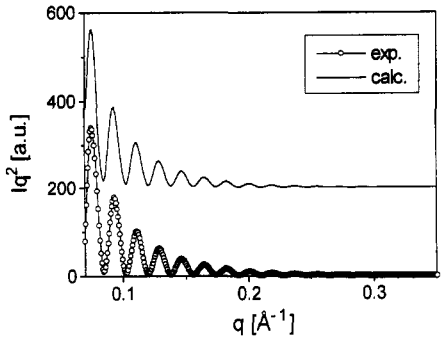

Figure 3. X-ray reflection curve of a 40-layer sample of IPC3.0 on silicon. Dots: experimental. Line: calculated. The calculated curve is shifted by 200 a.u. along the ordinate.

Table 1. Film Parameters of Multilayer Samples of IPC3.0, IPC2.9, IPC2.7, and IPC2.3 Obtained by X-ray Reflection[a]

	IPC3.0	IPC2.9	IPC2.7	IPC2.3
ϱ_p (e^{-1} Å^{-3})	0.29	0.31	0.33	0.33
E (Å)	383	352	335	316
d (Å)			16.7	15.8
σ_p (Å)	5	7	5.5	5
σ_s (Å)	5	5	5	5
ψ_1 (e^{-1} Å^{-3})			0.001	0.0059
static contact angle (deg)	92	90	85	75

[a] Each sample consisted of 40 monolayers. The contact angle of a water drop in contact with the topmost layer is also quoted.

the reagents. A completely alkylated product was obtained when the partially alkylated cellulose was subjected to a second alkylation run in a mixture of toluene and tetrahydrofuran with potassium *tert*-butylate as the base. The ds of the products was determined by elemental analysis, ^{1}H-NMR spectroscopy, and reductive cleavage of the polymer followed by GC/MS analysis of the products.[29]

For the characterization of cellulose ether multilayers by diffraction in reflection and transmission geometry, we concentrated on films of the peralkylated tri-*O*-isopentylcellulose (IPC3.0) which has a precisely defined repeating unit, unlike the partially substituted cellulose ethers.

Reflectivity. Investigation of multilayers of tri-*O*-isopentylcellulose (IPC3.0) by X-ray reflection generally shows Kiessig fringes which demonstrate the homogeneity of the film bulk and surface structure, but Bragg reflections which are normally expected of a periodical multilayer architecture are not observed. As an example, Figure 3 shows the X-ray reflection curve of a multilayer sample composed of 40 layers of IPC3.0 deposited on a silicon wafer.

Assuming an average electron density of 2.9 e^2/Å^3 of the multilayer, one obtains an overall film thickness E of 383 Å and surface roughness parameters of 5 Å for both interfaces by fit (Table 1). From the multilayer thickness of 383 Å and the number of layers deposited, a repeat distance of 9.58 Å/layer is obtained.

The lack of observable Bragg reflections may be due to a very flat repartition of the electron density along the normal to the layer plane.

In order to verify this point, we constructed a layered system with successive stacks of deuterated and nondeuterated isopentylcellulose. This layer system was subsequently analyzed by neutron reflection. In the case of a highly correlated multilayer structure, the alternating deposition should lead to a periodical scattering length density profile and consequently to Bragg reflections in the neutron reflectivity curve. If a disordered or uncorrelated layer structure is formed, the

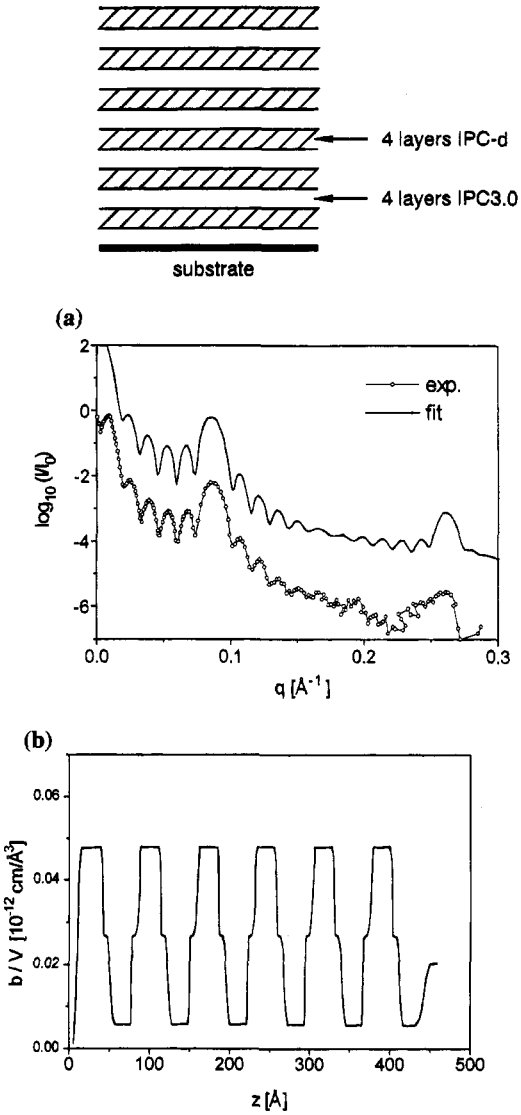

Figure 4. Neutron reflection curve of the depicted alternating layer sample constructed from IPC3.0 and IPC-*d* (a) and the scattering length density profile (b).

neutron reflection curve should lack Bragg reflections or exhibit specifically broadened peaks, indicating the paracrystalline deviation from order.

A superstructure of deuterated and nondeuterated material in layers was assembled by alternating deposition of sequences of 4 layers of IPC3.0 and IPC-*d* onto silicon, so that 6 periods of deuterated and undeuterated regions were obtained. Thus a superstructure of 6 repeating units composed of 48 individual monolayers was obtained as sketched in Figure 4a.

The X-ray reflection measurement of this alternating layer structure does not show Bragg signals—as in the case of multilayers of pure IPC3.0—but just Kiessig fringes from which an overall film thickness E of 432 Å was obtained. Therefore, the thickness per layer is 9.0 Å. This smaller value compared to the thickness of 9.58 Å determined from the multilayer if IPC3.0 discussed above may be due to altered transfer conditions, e.g., a slightly lower transfer pressure or a slightly slower ds for the deuterated sample.

The surface roughness σ_p of the polymer film was 7 Å; the roughness of the substrate σ_s was 5 Å by X-ray analysis. In contrast to the X-ray reflection experiment, the neutron reflection was performed under conditions close to total reflection so that dynamical effects had to be considered for evaluation.[31] The neutron reflectivity

curve of the alternating layer structure shows besides the Kiessig fringes 2 orders of a Bragg peak as shown by Figure 4a. Consequently, the sample is characterized by a highly ordered periodical layer structure.

A fit of the neutron reflectivity data results in a total film thickness of 432 Å, a periodicity of 72 Å, and roughnesses of 4.3 and 3.4 Å for the polymer surfaces at the substrate and toward air.

The periodicity of 72 Å reflects the lattice repeat produced by the sequence of four deuterated and four nondeuterated layers, each one contributing 9 Å to the total film thickness. The film thickness of 432 Å is consistent with the experimentally designed translational symmetry; in other words, it consists of 6 stacks of 72 Å thickness each. The overall film thickness and the roughnesses obtained by X-ray reflection and neutron reflection are the same within limits of error.

The existence of first- and third-order Bragg peaks in the neutron reflection curve indicates a well-defined long-range order with good correlation of individual layers in the superlattice. The absence of the second-order Bragg reflection points to a steplike distribution of scattering length density along the normal. In that case even coefficients of the scattering length Fourier expansion are equal to zero, leading to the absence of Bragg reflections of even indices.

A particular broadening of the Bragg reflection is not observed so that distortion effects of the second kind do not play a role; i.e., a long-range order with definite equilibrium positions of the layers is maintained.

A scattering length density profile obtained from the fit of the reflection curve, which is shown in Figure 4b, exhibits regions of higher scattering length density alternating with regions of lower density. A transition region of half a layer thickness with medium scattering length density may be caused by interdigitating side chains of neighboring layers.

With the neutron reflection data at hand it can be concluded that multilayers of tri-*O*-isopentylcellulose possess a very smooth and homogeneous, highly periodic film structure. The absence of Bragg diffraction peaks in the X-ray reflection can be explained by a very low electron density contrast along the surface normal of the multilayer structure.

It is, however, not possible to decide from these results whether a structure of double monolayers is formed or not. In the case of hairy rod multilayers from PG and PCPS a double layer structure is formed during deposition because of an asymmetrical side-chain distribution in the monolayer cause by polarization effects at the water surface. Therefore, a double layer formation in the cellulose ether layers is likely but cannot be proved by X-ray reflection because of the low amplitude of the electron density modulation.

Partially substituted isopentylcelluloses with free hydroxyl functions also proved to be suitable for multilayer preparation by the Langmuir–Blodgett technique. Obviously, the presence of not too many OH groups does not alter the transfer properties of the polymers.

Investigation of multilayers of isopentylcellulose with ds of 2.9, 2.7, and 2.3 by X-ray reflection revealed—as with multilayers of IPC3.0—a homogeneous film structure with a smooth surface. The X-ray reflection curves of samples of the three polymers, each one constructed from 40 monolayers, are depicted in Figure 5. The scattering curve of IPC2.3 exhibits a clear Bragg peak besides the Kiessig fringes. Even in the reflectivity curve of IPC2.7 a very weak Bragg peak is clearly visible. The parameters characterizing these films from fits of the reflectivity curves are summarized in Table 1.

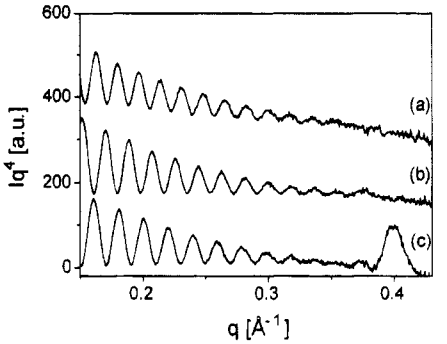

Figure 5. X-ray reflection curves of multilayered samples of 40 monolayers each of IPC2.9 (a), IPC2.7 (b), and IPC2.3 (c) on silicon.

Table 2. Film Parameters of the Molecularly Defined Superstructure from IPC3.0 and IPC-*d* Shown in Figure 4a As Obtained by X-ray Reflection and Neutron Reflection

	X-ray reflection	neutron reflection
ϱ_p (e^{-1} Å^{-3})	0.29	
b/V (Å^{-2})		3.4×10^{-6}
E (Å)	432	432
d (Å)	432	432
d (Å)		72
σ_s (Å)	5	3.4
σ_p (Å)	7	4.3

The multilayer thickness of the samples, which are equivalent in terms of the number of monolayers, decreases with decreasing degree of substitution of the cellulose ether. The repeat distance per layer, calculated from the overall film thickness E, is 8.8 Å for IPC2.9, 8.4 Å for IPC2.7, and 7.9 Å for IPC2.3. Whereas for the isopentylcellulose with a ds of 2.9 no Bragg reflection is observed, a reflection corresponding to double layer periodicities of 16.7 and 15.8 Å is detected in the cases of IPC2.7 and IPC2.3, respectively.

The surface roughness σ_p of 5–7 Å for the partially substituted cellulose ethers turned out to be independent of the degree of substitution.

The appearence of a Bragg reflection for the incompletely substituted derivatives can be explained by the change of electron density in the side-chain matrix which leads to increased electron density flucutation along the surface normal.

The static contact angle of a water drop at the surface of the multilayers from isopentylcellulose varies between 92° for IPC3.0 and 75° for IPC2.3 (Table 1) as a consequence of the increasing number of free OH groups in the uppermost layer. It may be hinted that the free OH groups at the surface could be used to modify the surface properties further by chemically attaching various functional groups.

Electron Diffraction. Two samples of the IPC3.0 were subjected to electron diffraction studies—a freshly prepared multilayer and an annealed (12 h at 150 °C) one, the latter enabling the determination of the crystalline structure of this cellulose ether.

A typical diffraction pattern obtained from a sample of 20 monolayers of tri-*O*-isopentylcellulose is shown in Figure 6a. There are basically two arc-shaped reflexes to be seen (the third is obviously a higher order of one of them), which indicate some preferential orientation of the macromolecules. However, these reflexes alone

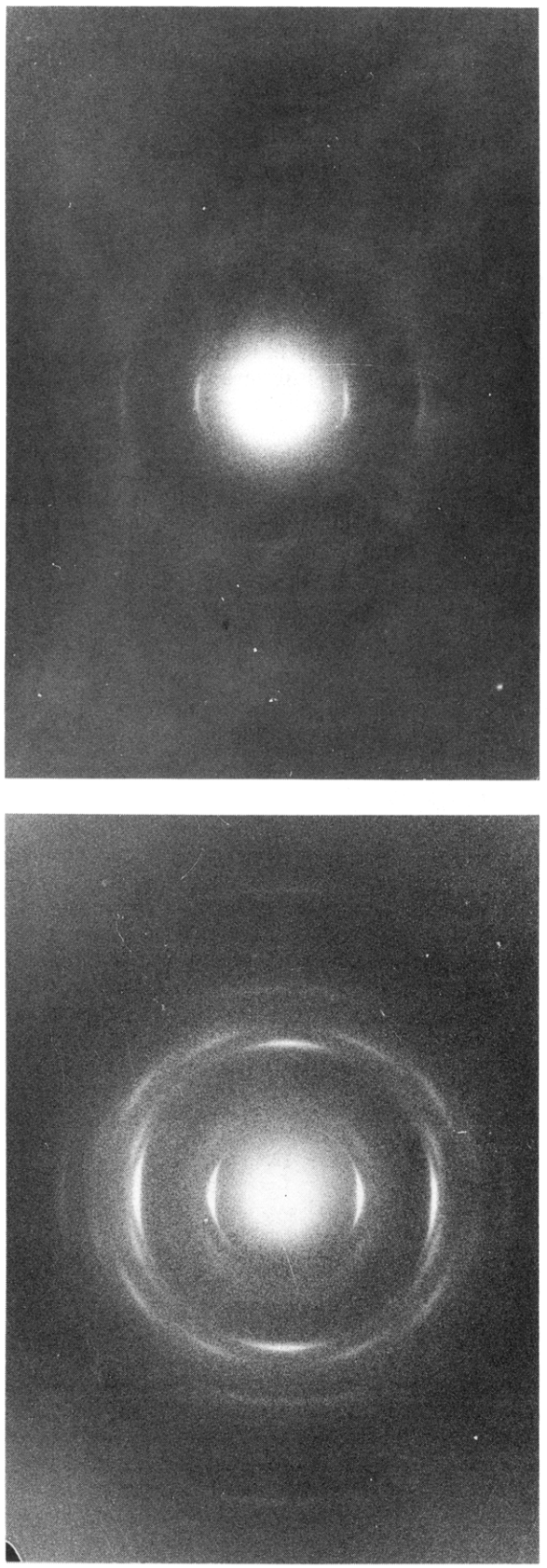

Figure 6. Electron diffractogram obtained from a sample consisting of 20 layers of IPC3.0: (a) original sample; (b) after annealing at 150 °C for 12 h.

are not sufficient to deduce unambiguously the trajectory of the polymer chain, as far as they correspond to lattice spacings of 10.4 and 5.1 Å, respectively, both equally well matching the average diameter of a single anhydroglucopyranose unit of about 5.15 Å and the chain repeat as well.

Table 3. Observed and Calculated *d* Spacings of an Annealed Multilayer Film of IPC3.0 (20 Monolayers)[a]

h	*k*	*l*		*d* (ber.) Å	*d* (exp.) (Å)
−1	1	0	+	11.53	11.58
0	2	0	*	10.47	10.51
−1	2	0		10.13	10.33
1	0	0		10.07	10.02
0	2	1	*	8.63	8.73
1	1	0		7.73	7.75
−1	3	0		7.78	7.75
0	3	1		6.34	6.30
−1	4	0		5.99	6.03
1	2	0		5.95	5.94
0	4	0	*	5.24	5.22
0	0	3	*	5.07	5.08
2	0	0		5.04	5.05
−2	4	0		5.06	5.02
0	4	1	*	4.95	4.95
−2	4	1		4.80	4.77
2	0	1		4.78	4.77
−1	4	2		4.71	4.74
−2	2	2		4.59	4.58
0	2	3	*	4.57	4.57
−1	2	3		4.54	4.57
2	−2	2		4.59	4.56
−1	0	3		4.53	4.54
0	4	2	*	4.31	4.32
0	5	1	*	4.04	4.03
0	6	0	*	3.49	3.49
0	0	6	*	2.54	2.53

[a] The indices are based on a monoclinic unit cell (see text). Asterisks denote signals which were obtained without tilting the sample. The signal labeled with + is observed only by X-ray reflection.

This problem can be solved by analyzing diffraction patterns of the annealed sample, one of which (at tilting angle 0°) is represented in Figure 6b. Besides the already known reflections from the previous figure, a great number of new ones is seen, indicating formation of a three-dimensional crystalline structure. In order to obtain diffraction patterns from further zones, the specimen was tilted with respect to the two main axes of the scattering pattern. The analysis of crystallographic data thus collected allowed the determination of the unit cell, which turned out to be a monoclinic one (γ unique) containing two chains. The lattice parameters were refined using a least-squares procedure. The results are as follows: $a = 11.52$ Å, $b = 23.97$ Å, $c = 15.22$ Å (chain direction), $\gamma = 119°$, $V = 3673.47$ Å^3, $z = 2$.

The density of this crystalline modification is calculated as 1.007 g/cm^3. Table 3 shows the observed and refined values of the interplanar spacings, corresponding to all reflexes detected, as well as their indexing based on the monoclinic unit cell. The rather peculiar observation that on the main meridian only 003 and 006 reflections are noticeable leads to the conclusion that the cellulose backbone adopts a 3-fold helical conformation. The data available cannot yet provide information about the sense of rotation, i.e., whether one has a 3_1 or 3_2 helix. This information can only be derived on the basis of a detailed conformation analysis. Such studies have been performed for a large number of cellulosics, and they show that for cellulose derivatives in general any kind of right-handed helix is not acceptable because of van der Waals contacts which are too short.[32] Therefore and in analogy the conclusion may be drawn, that in this case a 3_2 helix is formed as well.

The fact that a 003 reflection is observed in the scattering pattern of the freshly prepared multilayer system has to be considered as a strong indication that the helical conformation of the macromolecules is al-

ready existing on the water surface of the LB trough and may have been formed in the course of spreading the material and/or during compression of the monolayer.

By taking advantage of a very simple technique, it was possible to determine the polymer chain orientation with respect to the dipping direction, even though, due to lack of contrast and strong radiation sensitivity, direct TEM observation of the LB film was nearly impossible. Finder grids were used in the course of preparation, and care was taken, when the multilayer pieces were picked up, that the dipping direction was aligned parallel to the major axis of the grid. It was thus found that the main-chain trajectories coincide with the dipping direction within a deviation of ±12°. The orientational spread is most probably due to the conditions of the TEM sample preparation. Thus, the previous results by polarized FTIR spectroscopic measurements on LB films of cellulose ethers[20] could be substantiated, confirming that the chain trajectories become oriented into the dipping direction of the substrate during the LB process. Further analysis of the data reveals that the a-axis of the unit cell stands normal to the substrate, whereas the c-axis (chain axis of the cellulose ether) is parallel to the substrate plane.

There are substantial changes in density in the course of the annealing process. The crystalline sample of which the diffraction pattern is shown in Figure 6b has a crystalline density of 1.007 g/cm^3. However, samples freshly prepared and investigated by reflectometry (e.g., Figure 3) have densities of 0.85 g/cm^3. This change in density does not lead to the formation of macroscopic or microscopic pinholes or crazes within the layered sample.

5. Conclusions

Isopentylcellulose is demonstrated to be another example of the class of macromolecules denoted as "hairy rods" and, therefore, can be very well used to construct supramolecular architectures by the Langmuir–Blodgett technique. The fact that deuterated and nondeuterated isopentylcellulose could be deposited in specifically alternating structures proves the point and shows that self-diffusion of the constituent macromolecules is a very slow process, if it takes place at all. Note that several weeks have passed between preparation of the multilayered architecture of deuterated and nondeuterated molecules and its analysis by neutron diffraction. It is also worthwhile to emphasize the very small value of thickness per monolayer of 9.6 Å for the isopentylcellulose of ds 3 which decreases even further to ca. 8 Å for a sample of ds 2.3. Since the thickness is in the range where one expects tunneling phenomena to occur if a monolayer of this material is used as a separation between two metal or semiconductor electrodes, it is tempting to suggest experiments in this direction. An experiment along these lines of thought has been reported recently.[17,33] Another important feature is the observation that the spreading and transfer behavior in the LB process is not hampered by incomplete substitution. Thus, a fairly large number of free hydroxy groups (at ds 2.3) does not interfere with the attempt to build multilayered architectures. The relevance is, of course, that the surface polarity of the multilayer package can be controlled by the ds as indicated in Table 1. Together with the results from the preparation of the superficial architecture of deuterated and nondeuterated molecules, it is easy to see that a large number of interesting situations could be realized as, for instance, layered structures with a gradient of polarity normal to the layer plane.

We believe, therefore, that cellulose derivatives of the type discussed here significantly augment the toolbox of molecular architects and offer opportunities not available so far to create novel and useful structures by the LB process.

Acknowledgment. This work was supported by a grant from the German Bundesministerium für Forschung und Technologie (BMFT) in the framework of a project on ultrathin layers of polymers (UDS). The EM work was supported by another grant from BMFT in the framework of the Materials Research (MATFO) program. M.S. gratefully acknowledges a scholarship of the Stiftung Stipendienfonds of the VCI.

References and Notes

(1) Orthmann, E.; Wegner, G. *Angew. Chem.* **1986**, *98*, 1114.
(2) Sauer, T.; Arndt, T.; Batchelder, D. N.; Kalachev, A.; Wegner, G. *Thin Solid Films* **1990**, *187*, 357.
(3) Duda, G.; Schouten, A. J.; Arndt, T.; Lieser, G.; Schmidt, G. F.; Bubeck, C.; Wegner, G. *Thin Solid Films* **1988**, *159*, 221.
(4) Duda, G.; Wegner, G. *Makromol. Chem., Rapid Commun.* **1988**, *9*, 495.
(5) Mathauer, K.; Schmidt, A.; Knoll, W.; Wegner, G. *Langmuir*, in press.
(6) Embs, F.; Wegner, G.; Neher, D.; Albouy, P.-A.; Miller, R. D.; Wilson, C. G.; Schrepp, W. *Macromolecules* **1991**, *24*, 5068.
(7) Wegner, G. *Ber. Bunsen-Ges. Phys. Chem.* **1991**, *95*, 1326.
(8) Nizzoli, F.; Hillebrands, B.; Lee, S.; Stegeman, G. I.; Duda, G.; Wegner, G.; Knoll, W. *Mater. Sci. Eng.* **1990**, *B5*, 173.
(9) Wegner, G. *Mol. Cryst. Liq. Cryst.* **1992**, *216*, 7.
(10) Wegner, G.; Mathauer, K. *Mater. Res. Soc. Symp. Proc.* **1992**, *247*, 767.
(11) Schwiegk, S.; Vahlenkamp, T.; Xu, Y.; Wegner, G. *Macromolecules* **1992**, *25*, 2513.
(12) Ritcey, A.; Wenz, G.; Wegner, G. Presented at the IUPAC International Symposium on Macromolecules, Montreal, Canada, 1990.
(13) Katz, A.; Samwel, B. *Naturwissen* **1928**, *16*, 592.
(14) Borgin, K.; Johnson, P. *Trans. Faraday Soc.* **1953**, *49*, 956.
(15) Kawaguchi, T.; Nakahara, H.; Fukuda, K. *Thin Solid Films* **1985**, *133*, 29.
(16) Reidy, M.; Wenz, G.; Wegner, G., unpublished.
(17) Schaub, M. Ph.D. Thesis, University of Mainz, Mainz, FRG, 1993.
(18) Tieke, B. *Adv. Mater.* **1990**, *2*, 222.
(19) Tieke, B. *Adv. Mater.* **1991**, *3*, 532.
(20) Schwarz, R. Ph.D. Thesis, University of Mainz, Mainz, FRG, 1992.
(21) Embs, F. W.; Thomas, E. L.; Lieser, G.; Wegner, G. *Macromolecules*, in press.
(22) Rieutord, F.; Banattar, J. J.; Bosio, L.; Robin, P.; Blot, C.; de Kouchkovsky, R. *J. Phys. (Fr.)* **1987**, *48*, 679.
(23) Rieutord, F.; Benattar, J. J.; Rivoira, R.; Lepêtre, Y.; Blot, C.; Luzet, D. *Acta Crystallogr.* **1989**, *A45*, 445.
(24) Russell, T. P. *Mater. Sci. Rep.* **1990**, *5*, 171.
(25) Stamm, M. In *Physics of Polymer Surfaces and Interfaces*; Sanchez, I. C., Ed.; Butterworth–Heinemann: Manning, 1993.
(26) Stamm, M.; Majkrzak, C. F. *Polym. Prepr. (Am. Chem. Soc., Div. Polym. Chem.)* **1987**, *28*, 18.
(27) Kjaer, K.; Als-Nielsen, J.; Helm, C. A.; Tippmann-Krayer, P.; Möhwald, H. *Thin Solid Films* **1988**, *159*, 17.
(28) Kondo, T.; Isogai, A.; Ishizu, A.; Nakano, J. *J. Appl. Polym. Sci.* **1987**, *34*, 55.
(29) Mischnick, P. In *New Trends in Cyclodextrins and Derivatives*; Duchêne, D., Ed.; Editions de Santé: Paris, 1991; p 263.
(30) Zimmermann, H. *Liq. Cryst.* **1989**, *4*, 591.
(31) Anastasiadis, S. H.; Russell, T. P.; Satija, S. K.; Majkrzak, C. F. *J. Chem. Phys.* **1990**, *92*, 5677.
(32) Steinmeier, H. Ph.D. Thesis, Technical University Clausthal, 1988.
(33) Wegner, G. *Mol. Cryst. Liq. Cryst.* **1993**, *235*, 1.

MA9411742